Rheo-Optical Determination of the Interfacial Tension in a Dispersed Blend

Manlio Tassieri,[1] *Nino Grizzuti,**[1] *Francesco Greco*[2]

[1]Dipartimento di Ingegneria Chimica, Università di Napoli "Federico II", Piazzale Tecchio 80, I–80125 Napoli, Italy
[2]Istituto per la Tecnologia dei Materiali Compositi, ITMC, CNR, Piazzale Tecchio 80, I–80125 Napoli, Italy

Summary: In this work, we present two novel methods to determine the interfacial tension of a disperse polymer blend through rheo-optical measurements of flow-induced single drop distortions. A counter-rotating shearing device with transparent plates is used to measure drop distortions. The cell geometry allows for a top view of the deforming drop, i.e., along the velocity gradient direction. Such a view is the only possible option for all currently available commercial rheo-optical instruments. Two different quantities are monitored, namely, the drop axis along the vorticity direction, and the rotation period of the drop surface. We use drops of a polyacrilamide aqueous solution (a shear thinning liquid) immersed in a polyisobutene matrix. Experimental results are interpreted in terms of theories for Newtonian liquids, where the relevant parameter is the Capillary number. If an appropriate viscosity ratio is chosen, that accounts for the shear thinning behaviour of the drop phase, good agreement is found between measurements and theoretical predictions. As a result, a robust estimate of the blend interfacial tension, that makes use only of the information acquired from top view experiments, is obtained.

Keywords: blends; drop deformation; interfacial tension; microstructure; rheo-optics

Introduction

The flow induced deformation of a liquid droplet immersed into a liquid matrix is a widely studied problem[1]. In the Newtonian case, dimensional analysis shows that drop deformation can be described in terms of only two independent dimensionless parameters. One is the ratio between viscous and interfacial stresses, the Capillary number Ca, the other is the drop to matrix viscosity ratio, p. Thus, if a theory for drop deformation is available, comparison with experiments would allow for an estimate of the blend interfacial tension (appearing in Ca), once the viscosity of the

 DOI: 10.1002/masy.200350806

pure components is known[2].

In spite of the reduced number of parameters, shear flow deforms a droplet in a relatively complex way. Experiments as well as theoretical analyses show that the deformed droplet has a non-symmetric, fully three-dimensional shape that, at low *Ca*, approximates to an ellipsoid[3-7]. As a consequence, such a shape can only be reconstructed by performing optical observations along more than one direction.

Figure 1 depicts a deformed droplet as seen from the two relevant shear flow directions, namely, the vorticity direction (the so-called "side view", Figure1a), and the velocity gradient direction (the "top view", Figure1b). The side view gives direct access to two principal semi-axes, r_{MIN} and r_{MAX}, and to the drop inclination angle with respect to flow, φ. Measurements of side view drop deformation were first performed by Taylor in his pioneering work[3]. In more recent years, several investigators also adopted the same view, by designing their own home-made apparatuses[5,8-11].

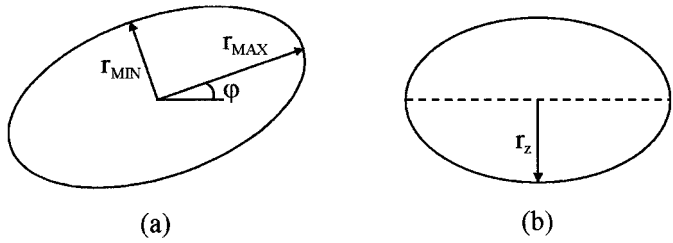

Figure 1. The two classical views of a deformed droplet. (a) side view; (b) top view. The flow direction is horizontal.

In all commercial rheo-optical apparatuses[12-14], however, optical observations can only be made along the velocity gradient direction. In such top view experiments, only the third principal semi-axis can be directly observed, the one along the vorticity direction, r_z (Figure1b). For an affordable determination of the interfacial tension, then, it would be highly desirable to develop a reliable methodology based on top view observations only, *plus* some convenient model describing drop deformation, including predictions of r_z as a function of *Ca* and *p*.

Attempts in this direction have already been made. Almusallam *et al*[15], for example, determined the interfacial tension of a Polybutadiene/Polydimethyilsiloxane blend by top view measurements

of a droplet subjected to a step shear deformation and subsequent relaxation. In their analysis, however, the drop inclination angle φ was required. This was determined by arbitrarily assuming affine deformation of the drop.

A further difficulty when dealing with drop deformation in polymer systems derives from their non-Newtonian character. While almost all currently available theories for drop deformation are for Newtonian systems, two main non-Newtonian features can affect the drop behaviour under flow. On the one hand, the elasticity of the components is known to produce significant deviations from the Newtonian case[16,17]. On the other hand, the shear rate dependency of the component viscosity, which in turn determines a varying blend viscosity ratio, can also have important consequences on drop evolution under flow. The latter aspect has never been studied in detail.

In this paper we perform top view observations of droplets of aqueous polyacrylamide solutions immersed in a polyisobutene matrix and subjected to a shear flow. The main objective of the work is to determine the blend interfacial tension by only using parameters that can be directly measured by top view experiments. Since the drop phase is characterized by a marked non-Newtonian behaviour, the possibility to adapt models for Newtonian emulsions to the case of a varying viscosity ratio is also considered. The paper is organized as follows. First, the theoretical background for shear-induced drop deformation is set, and the relevant model equations, that are necessary in order to interpret the experimental results, are introduced. Then, after describing the materials used to prepare the blends and the rheo-optical techniques, the experimental results and the methods to determine the interfacial tension are presented and discussed. Conclusions are drawn in the final Section.

Theoretical background

As mentioned in the Introduction, we will examine in this paper two different rheo-optical experiments for obtaining a measure of the interfacial tension under dynamical conditions. In one of these, we look at the drop axis r_z in the vorticity direction of a shear flow, and relate the length variations of this axis to the variation in the imposed shear rate $\dot{\gamma}$. In the other experiment, always under shear flow conditions, the rotation period T of a point at the drop surface is determined, again to relate the variations of this rotation period to $\dot{\gamma}$. In both the just mentioned cases, theoretical predictions do exist, for the r_z-axis and the period T, respectively, which are expressed

in terms of the Capillary number and the viscosity ratio:

$$Ca = \frac{\eta_m \dot{\gamma} r_0}{\sigma} \tag{1}$$

$$p = \frac{\eta_d}{\eta_m} \tag{2}$$

In Eqs (1) and (2) η_m and η_d are the matrix and droplet viscosity, respectively, r_0 the radius of the unperturbed droplet, and σ the interfacial tension. Hence, a separate knowledge of r_0, η_d, η_m, and $\dot{\gamma}$ allows one to infer the interfacial tension σ from measurements of r_z and T, and comparison with the theory. In this Section we report the needed formulae from theoretical analysis, and shortly discuss them.

Let us start with the r_z-axis determination. As it is well known, calculating the 3D-shape of a fluid drop immersed in another fluid flowing in an assigned way at infinity is a difficult task. The only available analytic results (for the Newtonian case) come from a perturbative procedure, with the Capillary number as the expansion parameter. For the shear flow case, which is the one experimentally investigated in the present paper, one obtains the following simple expression for the r_z-axis, up to second order in Ca[18]:

$$\frac{r_z}{r_0} = 1 - k(p) Ca^2 \tag{3}$$

with the coefficient $k(p)$ given by:

$$k(p) = \frac{42496 + 191824p + 261545p^2 + 111245p^3}{60480(1+p)^3} \tag{4}$$

(Notice that, from Eq.(3), the r_z-axis only deviates from the equilibrium drop radius r_0 at order Ca^2.) Thus, measuring the maximum drop dimension r_z in the z-direction leaves σ (contained in

Ca^2) as the only unknown quantity of Eq.(3). The interfacial tension is so obtained by performing a "top view" optical experiment, i.e., by looking at the deformed drop from the velocity gradient axis.

The same top view experiment can also lead to another determination of the interfacial tension, if a tracer particle is somehow placed on the drop interface. Indeed, in such a case, it is possible to measure the rotation period of the tracer particle around the drop. For the specific (and easiest) case of a particle moving on the shear plane, we can compare the experimental results to some well-known theoretical predictions available in the literature.

For $Ca \to 0$, which corresponds to an essentially undeformed droplet, the circulation period is found to be independent of the Capillary number and given by[3]:

$$m_0 = \frac{T\dot{\gamma}}{4\pi} = \frac{p+1}{\sqrt{p(p+2)}} \tag{5}$$

In Eq.(5), m_0 is the so-called "circulation number", and T is the revolution period. For $p \to \infty$, that is, for a hard spherical particle, Eq.(5) reduces to the well known result m_0=1, i.e., the sphere rotates with a frequency corresponding to one half of the shear rate. It should be stressed that Eq.(5) only holds for very low values of Ca. This point will be exploited later to obtain in any case an estimate for σ from Eq.(5).

An expression for m_0 that explicitly contains the Capillary number is that due to Cox[19]:

$$m_0 = \frac{p+1}{\sqrt{p(p+2)}} + \frac{19p(19p+16)}{4\left[(19p)^2 + (20/Ca)^2\right]}\left[25 - \frac{(p+1)(25p^2+50p-31)}{\sqrt{p^3(p+2)^3}}\right] \tag{6}$$

In this case, therefore, measurements of the rotation period T leave again σ (contained in Ca^2) as the only unknown quantity in Eq.(6). Hence, an "on-line" determination of the interfacial tension is feasible.

For the sake of completeness, let us add some comments on the above reported equations. First, concerning Eq.(6), we want to stress that the two terms in the RHS of the equation have not the same mathematical status. Indeed, the first term (independent of Ca) is the exact result from the

first-order theory by Taylor, while the second term, from Cox theory, is not rigorously deduced from the Newtonian fluid-dynamics of the single drop problem. In other words, Eq.(6) does not come from a general analytic solution of the drop problem, nor from a perturbative expansion in Ca (as it is the case, conversely, for Eq.(3) above). On the other hand, Eq.(6) is the only known expression for the rotation period T which accounts for the drop deformation. Actually, Taylor rigorous result (Eq.(5)) simply describes a decrease of T with increasing the shear rate $\dot{\gamma}$, whereas the complete Eq.(6) "corrects" (albeit in an approximate way) for the progressive increase of the interfacial area with $\dot{\gamma}$ itself.

Coming back to Eqs.(3) and (4), we should mention that the quadratic dependence of r_z on Ca has been experimentally shown elsewhere[20] to be in fact preserved up to moderate values of Ca (ca. 0.3, say, with $p\cong1$), which is a very favourable circumstance, in view of the inherent difficulties of measuring second-order quantities with sufficient accuracy. We should also notice here that the coefficient $k(p)$, as given in Eq.(4), is a rather weakly increasing function of the viscosity ratio, with an asymptote at $p\to\infty$ less than a factor 3 the value of k at $p=0$. This property of $k(p)$ will prove useful in the experiments reported in the present paper.

Finally, we have to remark that Eqs.(3)-(6) do in fact refer to a Newtonian system, but will be used in this work to deal with a non-Newtonian drop. In this respect, we remind the reader that the only non-Newtonian fluid-dynamic single drop problem that has been (perturbatively) solved is that for the constitutive case of the so-called "second-order fluids". Greco[17] demonstrated how the (order-of-magnitude) condition to have observable non-Newtonian effects under shearing flow condition is given by:

$$\left(\eta_d\dot{\gamma}\right)^2 \approx \frac{\sigma N_1}{r_0} \tag{7}$$

with N_1 the first normal stress difference of the droplet fluid. In view of the constitutive choice adopted in [17] (i.e., that of using the second-order fluid constitutive equation), however, Eq.(7) is only valid in a range of shear rates such that η_d stays constant, and N_1 is quadratic in $\dot{\gamma}$. Thus, when using shear-thinning fluids (as we do here, see below), we are in fact in a situation where the only existing non-Newtonian theory cannot be of help, not even in predicting (through Eq.(7))

whether non-Newtonian effects are observable or not. In the lack of anything better, then, we are compelled to use the Newtonian (approximate) formulae, Eqs.(3)-(6), in the rest of this paper.

Materials and methods

Aqueous solutions of polyacrilamide and pure polyisobutene (PIB) were used to prepare the model blend. A 5% wt solution of Separan AP30 (SAP30) was prepared by dissolving the necessary amount of polymer in bidistilled water, followed by gentle mixing with a magnetic stirrer at 50 rpm for several hours. The solution was then kept at rest for at least 24 hours, in order to remove air bubbles, and was sealed in glass containers. SAP30 concentration was periodically checked by dry residue measurements after vacuum oven treatment at 80°C. PIB (Parapol 1300, Exxon Co.) was used as received. For a simpler handling, PIB was preloaded into 10 cc hypodermic syringes, and it was centrifuged at 5000 rpm for 30 minutes in order to remove air bubbles.

The rheological properties of the two components were determined by means of a Rheometric DSR 200 rotational rheometer, equipped with cone and plate fixtures (plate diameter 40mm, cone angle 0.04 rad). A Peltier thermal unit guaranteed constant temperature measurements at 25°C with ±0.1°C accuracy.

Rheo-optical measurements of drop deformation were performed by means of a home-made counter-rotating device. The apparatus consists of two, independently motor-driven glass plates, that can rotate at constant angular speed. The liquid is loaded in the gap between the plates, and can be observed along the velocity gradient direction by means of a video camera connected to an *ad hoc* optical microscopy system. A more detailed description of the apparatus can be found elsewhere[21].

By suitably adjusting the oppositely directed rotation speeds of the two plates, any material point in the liquid can be deformed without being translated with respected to the microscope point of view. In this way, droplets of SAP30 solution in the PIB matrix could be observed for an indefinite time when submitted to a shear flow. In order to obtain well isolated, small SAP30 droplets, two loading procedures were used. In the first procedure, a PIB layer was applied on the bottom glass plate by means of the syringe. A thin thread of liquid SAP30 solution was gently extended on the PIB layer approximately along a plate radius. The thread was then covered by a second PIB layer

and the gap between the two plates was slowly set to its working position. A few minutes after loading, the SAP30 filament broke down into droplets by Rayleigh instability. Application of a moderate shear flow was used to displace the droplets from each other, so as to obtain a set of substantially isolated, non interacting SAP30 drops. In the second procedure, the gap between the two plates was completely filled with PIB. Then, a small droplet of SAP30 was injected by means of a microsyringe. If the injected drop had too large a diameter (exceeding about 100 μm), a strong shear flow was applied to the system in order to deform the drop into a filament, that would eventually breakup into smaller drops after cessation of flow.

After the loading procedure was completed, the experiment was started by applying the desired shear rate. Top view images of the deformed drops were video recorded and subsequently computer processed to extract the desired deformation data. All rheo-optical experiments were performed at the controlled ambient temperature of 25±1°C.

Experimental results and discussion

Figure 2 reports the viscosity of PIB and SAP30 as a function of shear rate at 25°C. PIB is a Newtonian liquid with a viscosity of about 95 Pa s. SAP30, conversely, shows a strong shear thinning behaviour, characterized by a power-law exponent n=0.29. The two viscosity curves intersect at a shear rate of about 0.7 s^{-1}. In view of the power law behaviour of SAP30, the viscosity ratio of the system can be cast in simple analytical form as:

$$p = 0.78\dot{\gamma}^{-0.71} \tag{8}$$

Drop deformation experiments were carried out in the shear rate window 0.1÷1 s^{-1}, thus resulting in a viscosity ratio ranging between 4 and 0.8. It should be mentioned that viscoelastic measurements (not reported here) show that PIB does not posses a significant elastic component, which is instead present in the case of SAP30. As pointed out in a previous Section, the effect of component viscoelasticity is not addressed in this work.

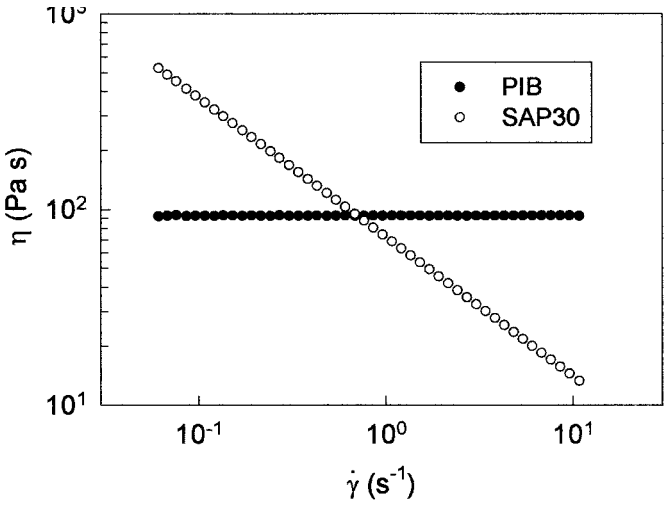

Figure 2. Viscosity of PIB and SAP30 as a function of shear rate at 25°C.

A first set of rheo-optical experiments concerns the measurement of steady-state drop deformation in shear flow. As the counter-rotating apparatus allows for a top view observation, the significant geometrical parameter to be measured is the drop semi-axis r_z. Figure 3 shows the drop deformation along the vorticity axis as a function of the shear rate for two SAP30 droplets of different radius. In Figure 3 the quantity $(r_z - r_0)/r_0^3$ is plotted as a function of the *square* of the shear rate. In fact, according to the theory presented previously, at low values of the capillary number r_z is expected to follow a quadratic dependence upon the shear rate. In particular, Eq.(3) indicates that, in the case of two Newtonian liquids, the following relationship holds:

$$\frac{r_z - r_0}{r_0^3} = \frac{\eta_m^2 k(p)}{\sigma^2}\dot{\gamma}^2 \qquad (9)$$

where k is the analytic function of the viscosity ratio given by Eq.(4).

Equation (9) predicts that, for a given pair of Newtonian liquids, the deformation measure in the LHS of the equation must be a universal function of the shear rate, independent of the droplet size.

Figure 3 confirms the validity of Eq.(9), as the experimental data for both drop sizes fall with good approximation on a single straight line.

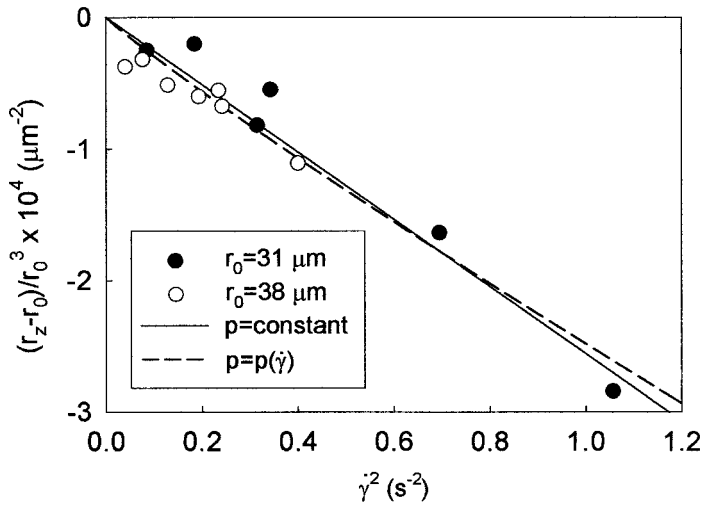

Figure 3. The deformation of two SAP30 droplets in PIB as a function of shear rate. See text for further details.

Figure 3 demonstrates the appropriate procedure to interpret drop deformation results when the optical observations are made along the velocity gradient direction. In particular, if all other quantities in the RHS of Eq.(9) are known, the experimental results can be used to determine the interfacial tension of the system. In the case of the PIB/SAP30 blend, however, this procedure could not be rigorously applied, as SAP30 is characterized by a shear thinning viscosity, in contrast with the assumption of Newtonian fluids dictated by the model. In particular, the non-Newtonian character of SAP30 shows up in the expression for the coefficient k, which is a function of the viscosity ratio.

In order to apply the model to the present situation, we make here the assumption that the model is still valid under a varying viscosity ratio. It should be noticed that, although arbitrary, such a hypothesis does not introduce significant numerical differences in the calculations. In fact, inspection of Eq.(4) shows that k varies only between 1.2 and 1.5 over the shear rate window

explored in the experiments.

Two different procedures have been applied in order to estimate the interfacial tension. In one case, a constant viscosity ratio, $\bar{p}$, is used. $\bar{p}$ is chosen as the simple arithmetic mean of the values assumed at the extremes of the experimental window:

$$\bar{p} = \frac{p(\dot{\gamma}_{min}) + p(\dot{\gamma}_{max})}{2} \qquad (10)$$

where $\dot{\gamma}_{min}$ and $\dot{\gamma}_{max}$ are the minimum and maximum experimental attained shear rates, respectively. In this case, i.e., with $p = \bar{p}$, Eq.(9) remains linear in the square of shear rate. The solid line in Figure 3 is indeed the linear fit of Eq.(9). Use of the constant viscosity ratio defined in Eq.(10) yields an interfacial tension of σ=6.8·10^{-3} N/m.

In the second fitting procedure, the viscosity ratio is allowed to change with shear rate. As a consequence, Eq.(9) is no longer simply quadratic in the shear rate, as k now depends on a varying p. The broken line in Figure 3 represents the best fit of Eq.(9) when $k(p)$ is calculated according to Eq.(4) with a varying p. In this case, an interfacial tension of σ=6.4·10^{-3} N/m results. Comparison of the two curves in Figure 3, and of the corresponding interfacial tension values, clearly shows that the agreement between experiments and model is not particularly sensitive to the choice of either a constant or a varying viscosity ratio.

A second set of rheo-optical experiments concerns the measurement of the rotation period of the droplet interface. Figure 4 shows a 38μm radius SAP30 drop in PIB undergoing a shear flow start-up. In Figure 4a the drop is at rest, and an air micro-bubble of about 2μm radius can be clearly seen on the right side of the interface. Such a micro-bubble can be obtained by the drop injection procedure outlined in the Materials and Methods Section. When the flow is started-up (Figure 4b) the air bubble starts traveling along the drop interface. The difference in refractive index between SAP30, PIB and air allows for a clear observation even when the bubble moves along the "hidden" side of the interface. At steady-state (Figure 4c) the drop reaches a constant deformation, and the bubble executes constant period revolutions around the drop interface. It should be also noticed that, at least in the case reported, the air bubble follows essentially the longest trajectory, that is, the one parallel to the flow direction.

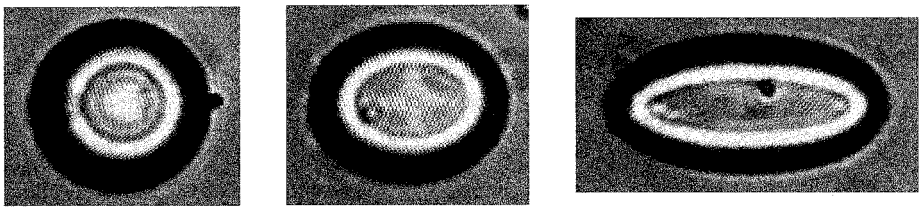

(a) (b) (c)

Figure 4. Top view of a SAP30 drop undergoing a shear flow start-up. The shear rate is 0.6 s^{-1} and the drop size is r_0=38μm. The direction of flow is horizontal. (a) quiescent drop, the air micro-bubble is on the right side; (b) the deforming drop during the transient flow, the air bubble is traveling along the bottom part of the interface; (c) the deformed drop at steady-state, the air bubble is now moving along the top part of the interface.

Assuming that the presence of the air bubble does not alter the flow conditions, and that the bubble itself remains attached to the interface, tracking the bubble motion allows for the measurement of the rotation period of the SAP30 droplet interface.

Figure 5 shows the interface rotation period T as a function of shear rate, as measured by air bubble tracking. T is a decreasing function of shear rate, because the droplet rotates faster as the shear rate is increased. Figure 5 also reports the comparison between the experimental results and the predictions of the available theories for droplet revolution time.

The dashed line in Figure 5 corresponds to Taylor's prediction, Eq.(5). In order to account for the non-Newtonian character of the viscosity ratio, an average value of p has been considered by using the same expression (Eq.(10)) already adopted to describe the drop deformation results. As expected, the prediction is only valid for low shear rates, corresponding to small values of the capillary number. The agreement between theory and experiments for $Ca \to 0$ is anyhow remarkable, as Eq.(5) does not contain adjustable parameters.

Although Taylor's theory does not contain any direct information on the interfacial tension, the observed deviation of the theory from the experimental results at increasing shear rates suggests a procedure to obtain a first, rough estimate of σ. Indeed, as said before, Taylor's theory is only applicable for Ca lower than some threshold value, Ca_t. At the same time, Figure 5 indicates a good quantitative agreement between theory and our data only for shear rates lower than a threshold value, $\dot{\gamma}_t \cong 0.35 s^{-1}$. Recent work on Newtonian drop deformation for viscosity ratios

around p=1[7] suggests $Ca_t \cong 0.1$. Collecting the above information leads to the following approximate relationship between Ca_t and $\dot{\gamma}_t$:

$$Ca_t = \frac{\eta_m \dot{\gamma}_t r_0}{\sigma} \cong 0.1 \qquad (11)$$

Equation (11) again contains σ as the only unknown parameter. Calculations yield σ=1.2·10^{-2} N/m, a value which is in semi-quantitative agreement with those obtained by the r_z measurements.

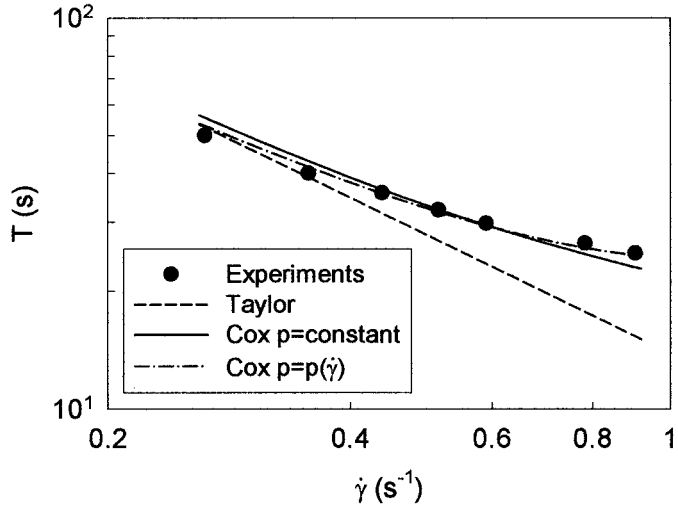

Figure 5. The period of rotation as a function of shear rate for SAP30 in PIB. The lines are the predictions of the Taylor and Cox models (see text).

A direct determination of the interfacial tension from the drop revolution results is obtained by fitting the Cox model, Eq.(6), to the experimental data, with the interfacial tension as the only unknown parameter. The solid line in Figure 5 represents the best fit of Eq.(6) when the average viscosity ratio $\bar{p}$ is used. Good agreement with the experimental results is found. Furthermore, the calculated value of interfacial tension, σ=6.5·10^{-3} N/m, is very close to that extracted from the r_z analysis. An even better agreement between theory and experiments is found (see dot-dashed

line in Figure 5) when the actual, shear rate dependent viscosity ratio is used in the Cox formula. In this case, a slightly higher interfacial tension results from the model regression results (σ=7.1·10^{-3} N/m), which is however still very similar to those obtained from drop deformation. As shown by Figure 5, the introduction of a varying viscosity ratio produces a slight improvement in the agreement between theory and experiments, and does not change significantly the calculated interfacial tension.

All values of interfacial tension calculated by the different experimental methods and with the different assumptions on the viscosity ratio are summarized in Table 1.

Table 1. Calculated values of interfacial tension from different experimental quantities

	r_z, $\overline{p}$	r_z, $p(\dot{\gamma})$	T (Taylor), $\overline{p}$	T (Cox), $\overline{p}$	T (Cox), $p(\dot{\gamma})$
σ (mN/m)	6.8	6.4	12	6.5	7.1

It can be concluded that, at least for the system investigated in this work, the analysis of top view optical observations leads to a robust estimate of the interfacial tension.

Conclusions

We have shown that top view observations of drop deformation in shear flow, which are typical of all commercial rheo-optical apparatuses, can be successfully used for the quantitative determination of the interfacial tension, once the appropriate deformation parameters are measured and adequately interpreted. In particular, for moderate values of the capillary number, measurements of the drop semi-axis along the vorticity direction, r_z, can be arranged in terms of a universal function of the applied shear rate. This allows for the determination of the blend interfacial tension, once the rheology of the two components is known. As an alternative, top view measurements of the droplet rotation period, which are available if a suitable tracer is deposited on the drop interface, can also be used for a quantitative estimate of the interfacial tension.

We have also shown that, at least for the polymer blend studied in this work, the shear thinning behaviour can be incorporated into models initially elaborated for Newtonian liquids, by allowing the viscosity ratio appearing in such models to depend on the shear rate, or alternatively by

defining a suitable mean viscosity ratio as an average over the experimentally accessed shear rate window. It seems feasible, therefore, at least from a practical point of view, to adapt the available Newtonian models to the case of varying viscosity blends.

The results of this work do not have the presumption to be at all exhaustive. As already pointed out before, the authors are aware that elastic phenomena (which are not considered here) could play an important role in the drop deformation of non-Newtonian systems. Efforts must be made to incorporate such effects in the presently available viscous models.

[1] C.L. Tucker III, P. Moldenaers, *Annu. Rev. Fluid Mech.*, **2002**, *34*, 177-210.
[2] I. Sigillo, L. di Santo, S. Guido, N. Grizzuti, *Polym. Eng. Sci.*, **1997**, *37*, 1540-1549.
[3] G.I. Taylor, *Proc. R. Soc. London*, **1932**, *A138*, 41-48.
[4] J. M. Rallison, *Annu. Rev. Fluid Mech.*, **1984**, *16*, 45.
[5] S. Guido, M. Villone, *J. Rheol.*, **1998**, *42*, 395-415.
[6] P.L. Maffettone, M. Minale, *Journal of Non-Newtonian Fluid Mechanics*, **1998**, *78*, 227-241.
[7] S. Guido, F. Greco, M. Villone, *J. Coll. Int. Sci.*, **1999**, *219*, 298-309.
[8] S. Torza, R.G. Cox, S.G. Mason, *J. Coll. Int. Sci.*, **1972**, *38*, 395-411.
[9] H.P. Grace, *Chem. Eng. Commun.*, **1982**, *14*, 225-227
[10] B.J. Bentley, L.G. Leal, *J. Fluid Mech.*, **1986**, *167*, 241-283.
[11] H. Yamane, M. Takahashi, R. Hayashi, K. Okamoto, *J. Rheol.*, **1998**, *42*, 567-580.
[12] Linkam CSS 450 shearing system technical notes, http://www.linkam.co.uk.
[13] Rheometrics Scientific OAMII technical notes, http://www.rheosci.com.
[14] Thermo Haake Rheoscope1 technical notes, http://thermo.com.
[15] A.S. Almusallam, R.G. Larson, M.J. Solomon, *J. Rheol.*, **2000**, *44*, 1055-1083.
[16] L. Levitt, C.W. Macosko, D.S. Pearson, *Polym. Eng. Sci.*, **1996**, *36*, 1647.
[17] F. Greco, *J. Non-Newt. Fluid. Mech.*, **2002**, submitted.
[18] F. Greco, *Phys. Fluids*, **2002**, *14*, 946-954.
[19] R.G. Cox, *J. Fluid Mech.*, **1969**, *37*, 601.
[20] S. Guido, F. Greco, *Rheol. Acta*, **2001**, *40*, 176-184.
[21] N. Grizzuti, O. Bifulco, *Rheol. Acta*, **1997**, *36*, 406-415.